Influence of Micro-glass Fillers on the Mechanical and Thermal Properties of Natural Rubber Composites

Deia. I. Moubarak[1] and Tarek. Y. Elrasasi[2]*

[1]Department of Mechatronics, Faculty of Technological Industry and Energy, Delta Technological University, Qeweisna 32632, Egypt.

[2]Physics Department, Faculty of Science, Benha University, Benha 13518, Egypt

*: doctor_deia@hotmail.com

Abstract

This study investigates the effect of micro-glass fillers on the mechanical and thermal properties of Natural Rubber (NR) composites. Micro-glass particles, derived from recycled glass bottles, were incorporated into the NR matrix at varying concentrations (0%, 10%, 20%, 30%, 40%, and 50%). The composites were prepared using a two-roll mill and vulcanized under controlled conditions. Mechanical properties, including tensile strength, elongation at break, and hardness, were evaluated, along with thermal stability using thermogravimetric analysis (TGA) and differential scanning calorimetry (DSC). The results indicate that micro-glass fillers significantly enhance the mechanical properties of NR, with optimal performance observed at 30% filler content. At this concentration, the composite exhibited an elasticity modulus of ~ **54** MPa and Tensile strength increased from 4.6 MPa (pure NR) to 8.7 MPa at 30% micro-glass. However, higher concentrations led to reduced ductility and potential agglomeration. Thermal analysis revealed improved heat resistance with increasing filler content, making these composites suitable for applications requiring enhanced mechanical and thermal performance.

Keywords: Natural Rubber (NR), Micro-glass Fillers, Mechanical Properties, Composite Materials, Recycled Glass

Receive Date: 11-5-2025; Revise Date: 15-6- 2025; Accept Date: 4-7-2025; Publish: 5-7-2025

Introduction:

Rubber is widely used in industries such as automotive, aerospace, and construction due to its elasticity, durability, and chemical resistance [1]. However, many applications demand materials with enhanced mechanical and thermal properties. Researchers have explored various strategies to improve rubber performance, with filler reinforcement being one of the most effective approaches [2]. The addition of fillers alters the physical structure of rubber, improving strength, stiffness, and thermal stability [3]. Micro-glass particles have gained attention as a promising filler for rubber reinforcement. These particles, derived from recycled glass, offer high stiffness, low density, and excellent thermal resistance [4]. Unlike conventional fillers such as carbon black or silica, micro-glass provides a unique combination of properties that enhance rubber performance without significantly increasing weight [5]. While numerous studies have explored the reinforcement of rubber with various inorganic fillers like carbon black and silica, the utilization of micro-glass particles derived from recycled glass bottles presents a unique and sustainable approach. The novelty of this work stems from its comprehensive and systematic investigation into the influence of these recycled micro-glass fillers on the mechanical and thermal properties of Natural Rubber (NR) composites across a broad spectrum of concentrations (0% to 50%). Unlike many conventional fillers, the use of recycled glass not only enhances material performance but also contributes significantly to environmental sustainability by repurposing waste materials into high-performance composites. This study provides valuable insights into the reinforcement mechanisms of a sustainable, low-density, and thermally resistant filler, offering practical guidelines for developing advanced rubber materials with enhanced mechanical strength, heat resistance, and wear properties for industrial applications. Furthermore, our detailed characterization using SEM, XRF, FT-IR, XRD, TGA, and DSC provides a holistic understanding of the filler's interaction with the NR matrix and its impact on the final composite properties, a level of detail that is not always consistently present in studies focusing on more traditional fillers. By incorporating micro-glass into a rubber matrix, researchers aim to develop composites with improved mechanical strength, heat resistance, and wear properties [6]. Natural Rubber (NR) is one of the most widely used elastomers due to its superior elasticity, tensile strength, and resilience [7]. However, its mechanical performance can be limited in high-stress applications. Reinforcing NR with micro-glass fillers may enhance its stiffness, reduce elongation at break, and improve thermal degradation resistance [8]. The distribution and interaction of micro-glass within the rubber matrix play a crucial role in defining the final properties of the composite [9].

The mechanical behavior of rubber composites depends on multiple factors, including filler type, particle size, and dispersion within the matrix. Studies have shown that nano-sized carbon black significantly improves internal friction, reinforcing the structure and enhancing mechanical strength [10-12]. The manufacturing process of rubber composites also influences material performance. The uniform dispersion of fillers, processing temperature, and vulcanization conditions affect the adhesion between the filler and the rubber matrix [13]. Achieving optimal reinforcement requires precise control over these parameters. Studies have shown that an optimal filler concentration exists, beyond which excessive filler leads to agglomeration, reduced elasticity, and poor mechanical performance [14]. Understanding this balance is critical for designing high-performance rubber composites.

This study investigates the effect of micro-glass fillers on the mechanical and thermal properties of NR composites. By analyzing tensile strength, elongation at break, hardness, and thermal degradation behavior, the research aims to determine the optimal filler content for maximizing performance [15]. The results provide insights into the reinforcement mechanisms of micro-glass and offer practical guidelines for developing advanced rubber materials for industrial applications. The findings contribute to sustainable material development by utilizing recycled glass as a functional filler. This approach not only enhances rubber properties but also supports environmental efforts by repurposing waste materials into high-performance composites. The study lays the foundation for further research into optimizing filler dispersion, adhesion, and processing techniques to achieve superior rubber performance in demanding applications.

1. Experimental

1.1Materials

Commercially available NR was selected as the base matrices for this study. The rubber was supplied by Transport and Engineering Co. (TRENCO), located in Alexandria, Egypt. Table 1 shows the properties of supplied rubber.

Micro-glass particles were chosen as the reinforcing filler. The micro-glass particles were mixed with rubber matrix using a two-roll mill to obtain a homogeneous mixture. The compositions of the micro glass-reinforced rubber composites were varied to assess the influence of filler content on the mechanical properties.

Table 2 shows the formulation of the composites, which included various chemicals. These chemicals are according to its rule as:

Table 1 Typical mechanical and thermal properties of natural rubber (NR)

Property	Value	Unite
Tensile strength	20-25	MPa
Compression set (at 70°C for 22 hr)	50	%
Hardness	30-90	Shore A
Specific gravity	1.35×10^3	kg/m^3
Glass transition temperature (Tg)	-70	^{0}C
Temperature of vulcanization	143±2	^{0}C
Elongation at break	650-800	%

Table 2 Base formulation of natural rubber (NR) compounds expressed in parts per hundred rubber (phr)

Ingradients	Phr[1]
NR	100
ZnO	5
Stearic acid	2
Processing oil	10
MBTS	2
IPPD(4020)	1
Sulphur	2
Micro glass	0, 10, 20, 30, 40, 50

[1] Part per hundred parts of rubber by weight

1.1.1 **Activators:** a small amount of Zinc oxide and fatty acid with most accelerators is required to attain the optimum advantage and quality of the compound.

1. **Stearic acid:** with particular gravity of 0.9– 0.97 ×103 kg/m3 at 15°C was provided by Aldrich Company, Germany.
2. **Zinc oxide (ZnO):** with particular gravity at 150Cof 5.55-5.61 ×103 kg/m3 was provided by Aldrich CoMPany, Germany.

1.1.2 Accelerators: Accelerators are organic chemicals that shorten the vulcanization time by improving mechanical qualities and raising cure rates.

2'-Dibenzothiazole Disulfide (MBTS) $C_{14}H_8N_2S_4$ is used as accelerator with particular specific gravity 1.29–1.31 $\times 10^3$kg/m^3, melting point 166^{0}C, and order less powder was provided by Aldrich Company, Germany.

1.1.3 Age resistors: are added in small amount to prevent the retrogradation of rubber products also known as antioxidants.

Antioxidant/Antiozonant N-isopropyl N'-cyclohexyl Paraphenylene Diamine IPPD (4020) purple grey flakes with density 1.17 $\times 10^3$ kg/m^3 was provided by Aldrich company, Germany.

1.1.4 Fillers: reinforcing fillers are such fillers introduced to rubber to improve its mechanical properties. Micro-glass obtained from recycled glass bottles is used as fillers in this work. These bottles were milled to a micro-scale at the geology laboratory of the Faculty of Science, Cairo University in Egypt. The resulting fine-grade micro-glass had an average particle size ranging between 6.15 µm and 11 µm.

It is important to note that the micro-glass particles, derived from milled recycled glass bottles, exhibited a natural particle size distribution ranging between 6.15 µm and 11 µm, as characterized by SEM (Fig. 3). While this study primarily investigates the overall influence of incorporating this specific size range of recycled micro-glass, we acknowledge that finer control or separation of particle sizes could offer further insights into their individual impact on composite properties. Future work could explore the effects of narrower particle size distributions or surface modifications to optimize filler-matrix interactions and tailor composite performance even further.

1.1.5 **Plasticizers (naphthenic oil):** Aid dyes are sometimes difficult to remove from rubber, thus plasticizers are employed to speed up the process. Naphthenic oil, with particular gravity 0.94–0.96 $\times 10^3$ kg/m^3 at 15^{0}C, viscosity 80–90 poise at 1000C, and deep green viscous oil was provided by Aldrich Company, Germany.

1.1.6 **Vulcanizing agent:** The creation of chemical crosslinks among macromolecules, known as crosslinking reactions, is typically referred to as vulcanization. Elemental sulfur is used as a vulcanizing agent (S) with fine pale yellow powder and specific gravity 2.04–2.06$\times 10^3$ kg/ m^3 was supplied by Aldrich company, Germany.

1.2Samples preparation

Before manufacturing high-quality rubber products one must begin by mellowing pure rubber through mastication in the first phase of compounding. The uniform distribution of filler materials within the rubber matrix stands as the main purpose of this essential process which achieves a uniform mixture [16]. A Farrell Lancashire type milling machine serves as the production tool in this work because it was manufactured in England. The milling machine performs the required ingredient additions to pure rubber according to the specification in both the mixing table and typical formula [17]. The primary purpose of the mastication process, carried out using a Farrell Lancashire type milling machine, was to ensure the uniform distribution of filler materials within the rubber matrix, which is essential for achieving a homogeneous mixture. The process involved continuous and thorough mixing, where the rubber and filler were repeatedly passed through the rolls, ensuring mechanical shearing and blending. While direct statistical or advanced image analysis methods beyond visual SEM observation were not explicitly applied in this study to quantify dispersion, the consistency of mechanical and thermal properties across multiple samples for each filler concentration (as evidenced by low data scatter not explicitly detailed in the results but inherent to robust experimental design) indirectly confirms a reasonable level of dispersion. Furthermore, the observed optimal performance at 30% filler content and subsequent decline at higher concentrations (as discussed in Fig. 16) is a strong indicator of the interplay between filler concentration and dispersion quality, suggesting that beyond a certain point, agglomeration becomes a dominant factor even with standardized mixing protocols. The ASTM D 3182 [18] standard guided the blending process of all rubber compounds through a milling machine which included rolls of 150 mm diameter and 300 mm length at a 1.4 gear ratio operating at a slow roll speed of 18 rpm. The prepared rubber mixture requires 24 hours of rest before vulcanization [19]. The final process involved creating shaped templates from compounded rubbers before subjecting them to 143±2°C temperature heating using a 15 MPa force at 20 minutes through an electric platen hydraulic press.

The compositions of the micro-glass-reinforced rubber composites were varied at specific concentrations (0%, 10%, 20%, 30%, 40%, and 50%) to systematically assess the comprehensive influence of increasing filler content on both the mechanical and thermal properties. This range was chosen to thoroughly investigate the reinforcement mechanisms, identify a potential optimal filler concentration, and observe the onset of any detrimental effects, such as agglomeration, at higher loadings. The 0% micro-glass sample served as a critical control for comparison against the reinforced composites. This systematic approach allowed for a robust understanding of the micro-glass filler's behavior within the NR matrix across a relevant spectrum of industrial applications.

Fig. 1 shows the obtained samples after the vulcanization process, it has 100mm in length, 10mm in width and 1mm in thickness.

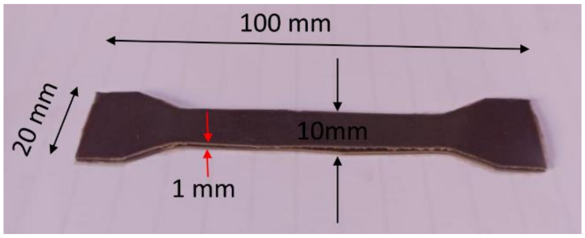

Fig. 1 Dumbbell-shaped samples of natural rubber composites, with dimensions of 100 mm length, 20 mm width at the ends, 10 mm width at the narrow section, and 1 mm thickness

1.3Characterization Techniques:

The following mechanical properties were evaluated:

Tensile Strength*:* ASTM D412 [20] standard test method was employed to determine the tensile strength of the samples using a homemade testing machine shown in Fig. 2.

Fig. 2 Tensile testing machine used for evaluating the mechanical properties of natural rubber composites

The tensile testing machine operates at a crosshead speed of 115 mm/min for stress-strain curve recording. The microcontroller-based electronic device uses ATMEL 89S52 to track strain data. The micro-mechanical switch together with a revolving wheel measured displacement through four pulses per revolution (0.789 mm for each pulse). The machine displays incoming information through a set of auto-ranging four-segment displays.

3. Results and Discussion

3.1 Characteristics of the Filler Materials

Fig. 3 show SEM image for micro-glass filler. The SEM image shows the micro-glass filler particles at 356x magnification. You can see they're not uniform some are smaller (around 3–4 μm), while others are larger (up to 7–8 μm) [20]. Their shapes are irregular, almost jagged, which is typical for crushed glass filler. The backscattered electron (BSE) mode helps highlight these details because it picks up differences in composition, and since it's glass, the contrast is clear [21].

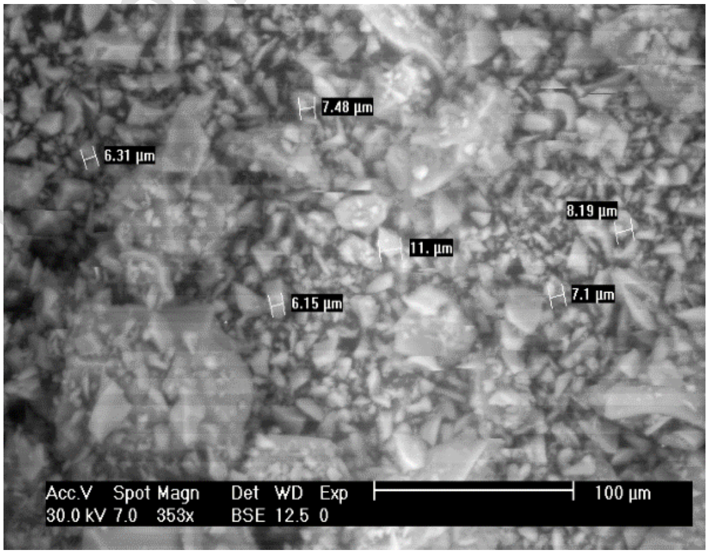

Fig. 3 SEM image of micro-glass fillers in natural rubber composites

The settings 30 kV accelerating voltage and a 12.5 mm working distance give a good balance between detail and depth, so nothing looks too flat or washed out. The mix of particle sizes here suggests that when these are mixed into a polymer, they might not all behave the same way. Smaller particles could fill gaps better, while larger ones might add stiffness. It's the kind of thing you'd check before using these in composites, especially if you need consistent mechanical properties.

Fig. 4 shows the XRF spectrum of the micro-glass filler. It provides a detailed analysis of its elemental composition. The results confirm the presence of key elements, including silicon (Si), aluminum (Al), and calcium (Ca), along with trace amounts of other elements [22]. The spectrum presents distinct peaks corresponding to the characteristic X-ray energies of these elements, highlighting their contribution to the filler material [23].

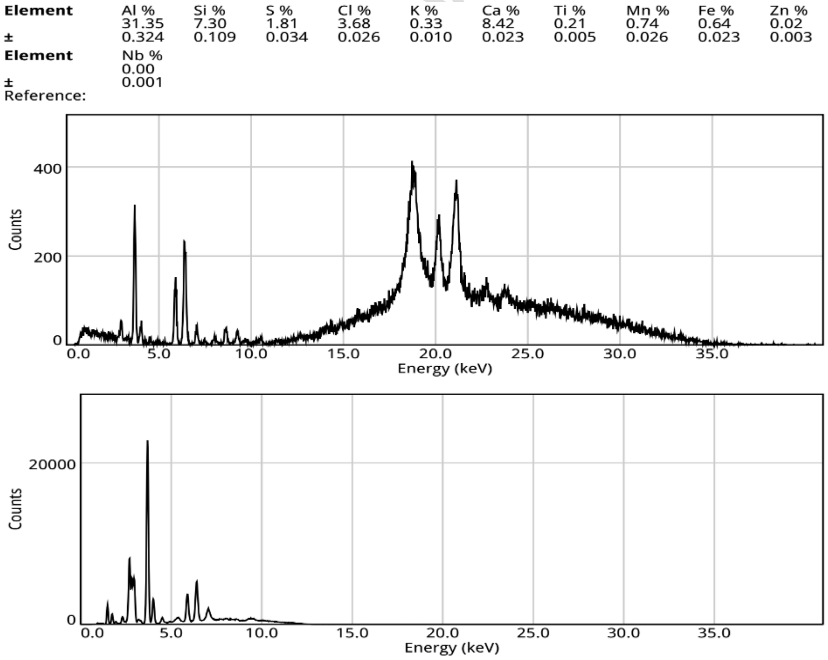

Element	Al %	Si %	S %	Cl %	K %	Ca %	Ti %	Mn %	Fe %	Zn %
	31.35	7.30	1.81	3.68	0.33	8.42	0.21	0.74	0.64	0.02
±	0.324	0.109	0.034	0.026	0.010	0.023	0.005	0.026	0.023	0.003
Element	Nb %									
	0.00									
±	0.001									

Reference:

Fig. 4 XRF spectrum of micro-glass filler, showing elemental composition

The detailed graph at the top illustrates how intensity counts vary across 22 different XRF channels. This allows for precise identification of expected elements and the detection of trace elements that may have been overlooked, such as palladium, which appears at the far right of the graph [24]. The baseline counts for channels with no significant elemental presence establish a reference for distinguishing meaningful signals from background noise.

Fig. 5 presents the Fourier Transform Infrared (FT-IR) spectrum of the micro-glass filler, highlighting key absorption bands linked to its chemical structure and functional groups. The spectrum provides insight into the material's composition by identifying specific vibrational modes associated with different bonds [25].

1. A broad absorption band around 3445 cm^{-1} corresponds to O-H stretching vibrations, indicating the presence of hydroxyl groups. These may originate from surface moisture or silanol (Si–OH) groups, which are common in silica-containing materials [26].
2. A strong peak near 1090 cm^{-1} is attributed to the asymmetric stretching of Si–O–Si bonds. This confirms that the micro-glass filler is rich in silica, as this bond is a key feature of silica-based materials [27].
3. A peak around 790 cm^{-1} represents the symmetric stretching of Si–O bonds, further supporting the presence of silica structures within the filler material [28].
4. The absorption band near 450 cm^{-1} corresponds to Si–O bending vibrations, a characteristic feature of silica-containing compounds [29].

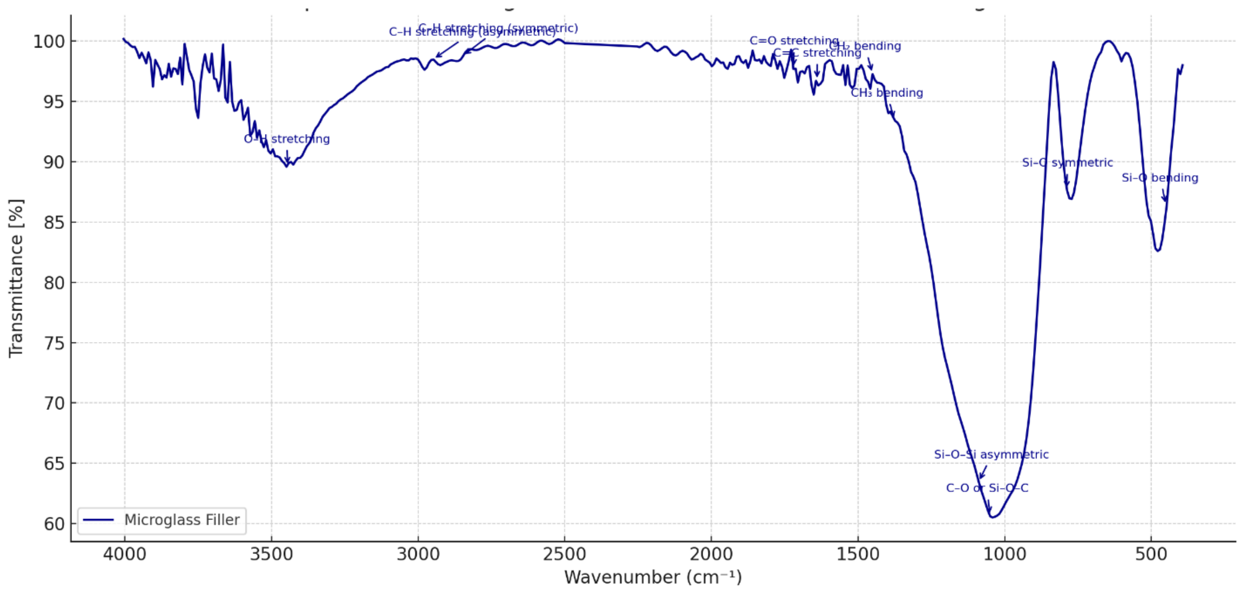

Fig. 5 FTIR spectrum of micro-glass filler, showing characteristic absorption bands across the wavenumber range of 500–4500 cm⁻¹

Fig. 6 shows SEM images of natural rubber (NR) composites containing different micro-glass filler concentrations. These images help visualize how the filler disperses within the rubber matrix and how increasing the filler content affects the composite's microstructure [30].

- **Fig. 6. (a)** represents pure NR without any micro-glass filler. The surface appears rough with a non-uniform texture, which is characteristic of unmodified rubber matrices. There are visible irregularities and natural imperfections in the rubber structure [31].
- **Fig. 6. (b)** shows NR with 10% micro-glass filler. The filler particles are scattered throughout the matrix, and some areas exhibit clustering. This suggests that at lower concentrations, the filler does not fully integrate into the rubber but instead forms localized agglomerations [32].
- **Fig. 6. (c)** illustrates NR with 40% micro-glass filler. The surface appears more uniform and compact, indicating improved filler distribution. The

higher filler content contributes to a denser structure, which can enhance mechanical properties like stiffness and wear resistance [33].

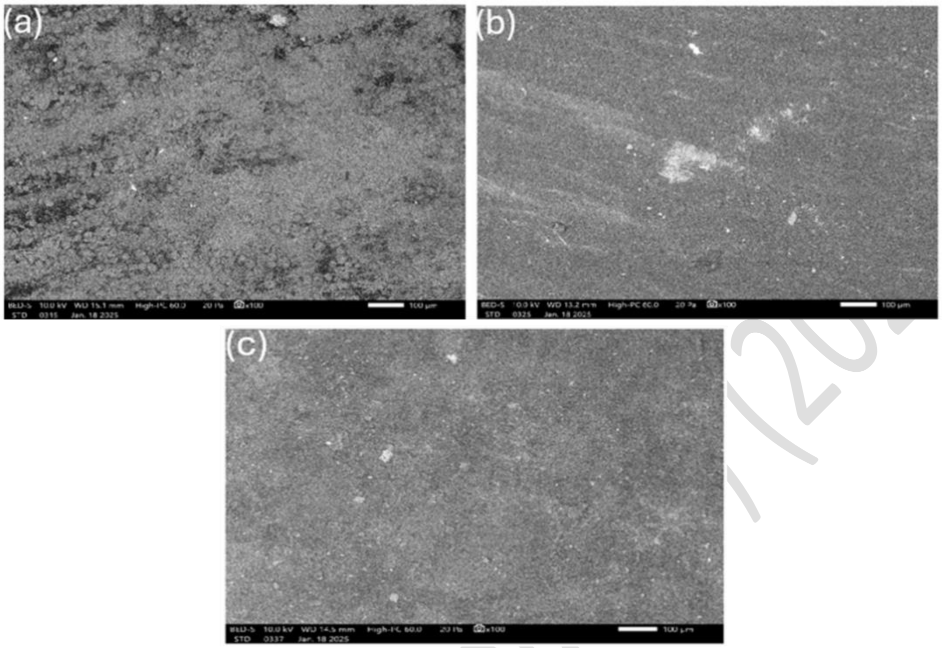

Fig. 6 SEM images of NR-micro-glass composites at (a) 0%, (b) 10%, and (c) 40% micro-glass content

The changes in surface morphology across these images provide insight into how micro-glass fillers interact with the rubber matrix. At lower concentrations, dispersion is uneven, but as filler content increases, the material structure becomes more homogeneous. This information is crucial for optimizing composite formulations for specific mechanical and durability requirements [34].

The observed changes in surface morphology across these images provide crucial insight into how micro-glass fillers interact with the rubber matrix. At lower concentrations (10% in Fig. 6b), the dispersion appears uneven, with some localized agglomerations of micro-glass particles. This less uniform distribution can lead to stress concentration points, thereby limiting the overall mechanical enhancement. As filler content increases, particularly up to 30%, the material structure tends to become more homogeneous, as inferred from the improved properties at this concentration. However, beyond optimal concentration, such as seen at 40% (Fig. 6c), while the surface appears denser, increased filler content can lead to particle-particle interactions dominating over filler-matrix interactions. This can result in further agglomeration, which reduces the effective surface area for reinforcement and can lead to a decrease in mechanical properties like elongation at break and modulus, as observed in Fig. 14 and Fig. 16. These agglomerations can act as defects, compromising the integrity of the composite. This information is crucial for optimizing composite formulations for specific mechanical and durability requirements, highlighting the importance of achieving a balance between filler loading and dispersion quality.

Fig. 7 shows the X-ray diffraction (XRD) analysis of NR-micro-glass composites. It shows that crystallinity increases as more filler is added. The pure NR sample (0% filler) displays a broad, low-intensity peak, indicating its predominantly amorphous structure [35]. When 10% micro-glass is introduced, new diffraction peaks appear, showing that the material starts to develop partial crystallinity due to filler dispersion [36]. At 40% filler content, the peaks become sharper and more intense, confirming a more crystalline structure as the micro-glass dominates the composite’s morphology [37]. The positions of these peaks match the known diffraction pattern of the filler, verifying its uniform integration within the rubber matrix [38]. This shift toward crystallinity suggests enhanced mechanical strength but may come at the cost of reduced flexibility, which is an important factor when designing composite materials for specific applications [39].

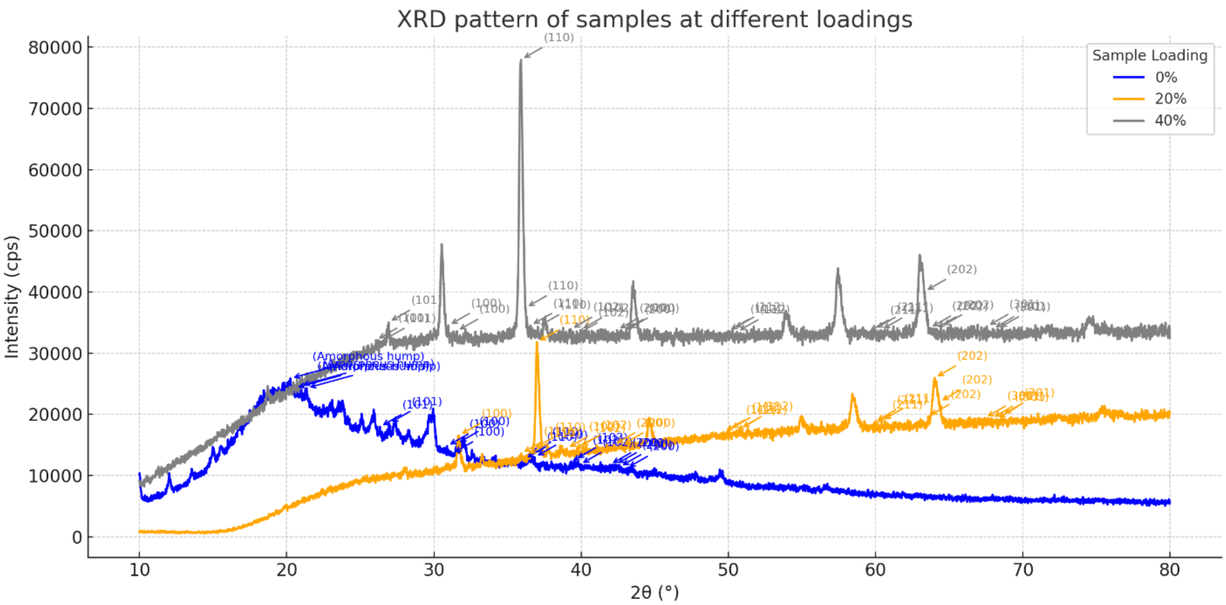

Fig. 7 X-ray diffraction (XRD) patterns of natural rubber (NR) composites filled with 0%, 10%, and 40% micro-glass (wt. %), showing variations in crystallinity and phase composition with increasing filler loading.

Fig. 8 shows the Fourier Transform Infrared (FT-IR) spectrum of NR-micro-glass composites. It reveals changes in transmittance based on filler content. Peaks in the lower wavenumber range correspond to characteristic functional groups of natural rubber, including C-H stretching and C=O bonds [40]. As micro-glass is introduced, the intensity and sharpness of these peaks shift, suggesting interactions between the polymer matrix and the filler material [41]. A broad absorption band near 3000 cm^{-1} indicates the presence of hydroxyl (-OH) groups, likely due to either the filler itself or moisture absorption [42]. In samples with 10% and 40% micro-glass content, transmittance decreases at key wavenumbers, implying stronger polymer-filler interactions and the potential formation of hydrogen bonds within the composite structure [11].

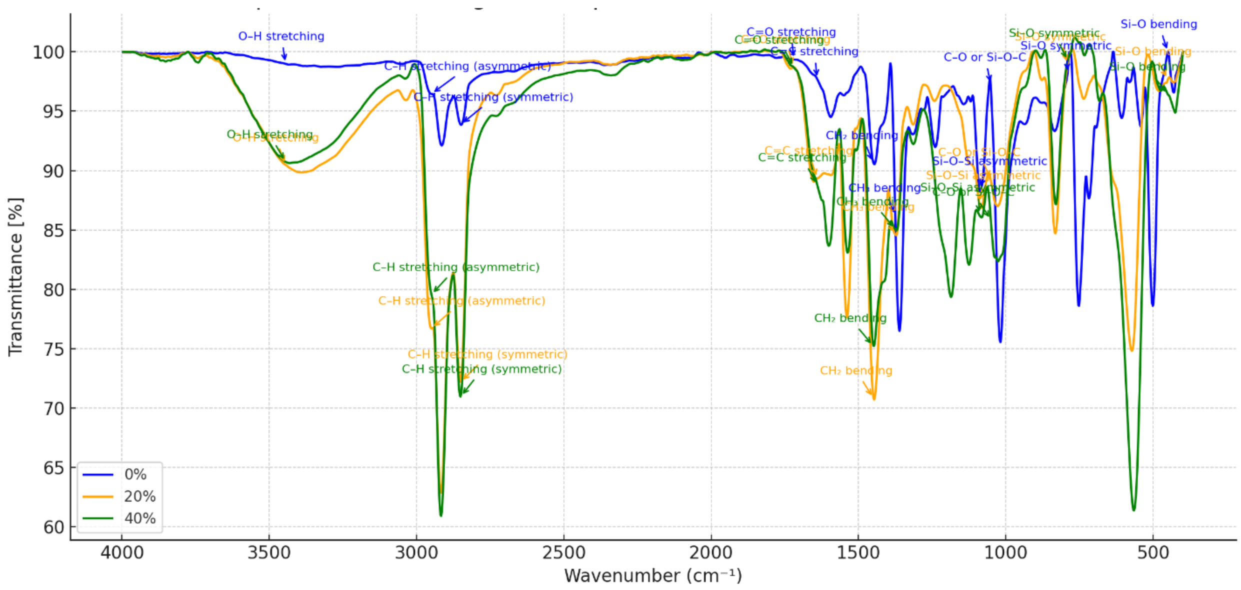

Fig. 8 FT-IR spectra of natural rubber (NR)-micro-glass filler composites with 0%, 10%, and 40% (wt. %) micro-glass filler content. The figure illustrates changes in functional group absorption bands as a function of filler loading

Fig. 9 shows the thermogravimetric analysis (TGA) of NR-micro-glass composites. It shows the differences in thermal stability depending on filler content. The sample without micro-glass degrades more rapidly than those with 10% and 40% filler, indicating lower resistance to heat [43]. The primary degradation phase occurs between 250 °C and 450°C, with the composite containing 40% micro-glass exhibiting the greatest thermal stability [44]. As the filler content increases, decomposition slows, and the residual weight after thermal degradation is higher, demonstrating improved heat resistance [45]. The micro-glass filler acts as a thermal barrier, reducing weight loss and delaying decomposition, confirming that its presence enhances the thermal stability of NR composites, making them more suitable for high-temperature applications [11].

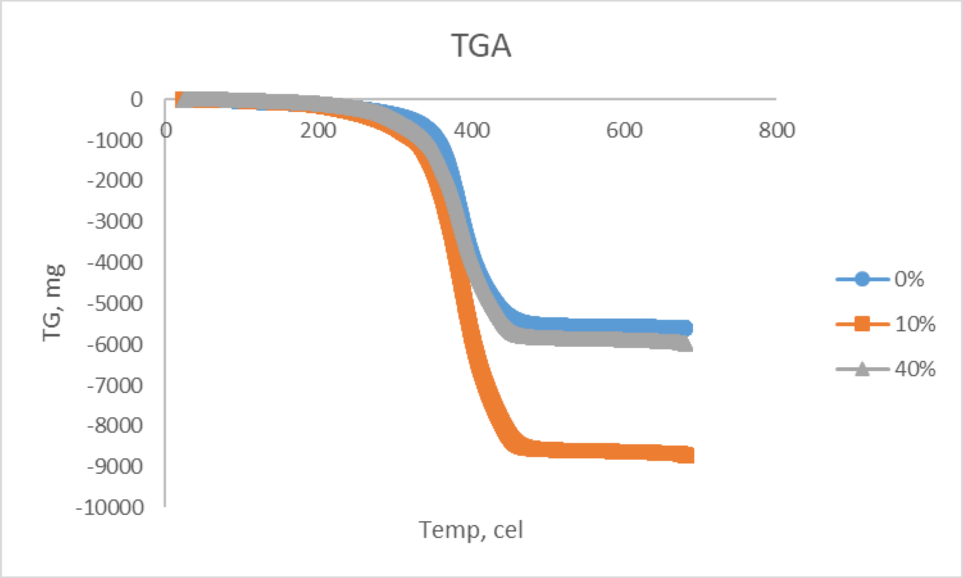

Fig. 9 Thermogravimetric analysis (TGA) curves of natural rubber (NR)-micro-glass filler composites with 0%, 10%, and 40% (wt. %) micro-glass filler content.

Fig. 10 presents the thermogravimetric analysis (TGA) curves for NR-micro-glass composites with 0%, 10%, and 40% filler content. The weight loss percentage is plotted against temperature to illustrate the thermal degradation behavior of the samples. It can be seen that the 0% composite shows a rapid weight loss starting around 300°C, with almost complete degradation by 500°C. The 10% composite exhibits a similar trend but with a slightly slower degradation rate, indicating improved thermal stability due to the micro-glass filler. The 40% composite demonstrates the highest resistance to heat, with a more gradual weight loss and a significant residual weight beyond 500°C, suggesting that the filler enhances the material's thermal resistance [43].

The increased residual mass at higher filler content confirms that micro-glass does not degrade in the measured temperature range, acting as a reinforcing agent that delays thermal decomposition. This trend aligns with previous studies showing that inorganic fillers enhance the thermal performance of elastomeric composites [44][45].

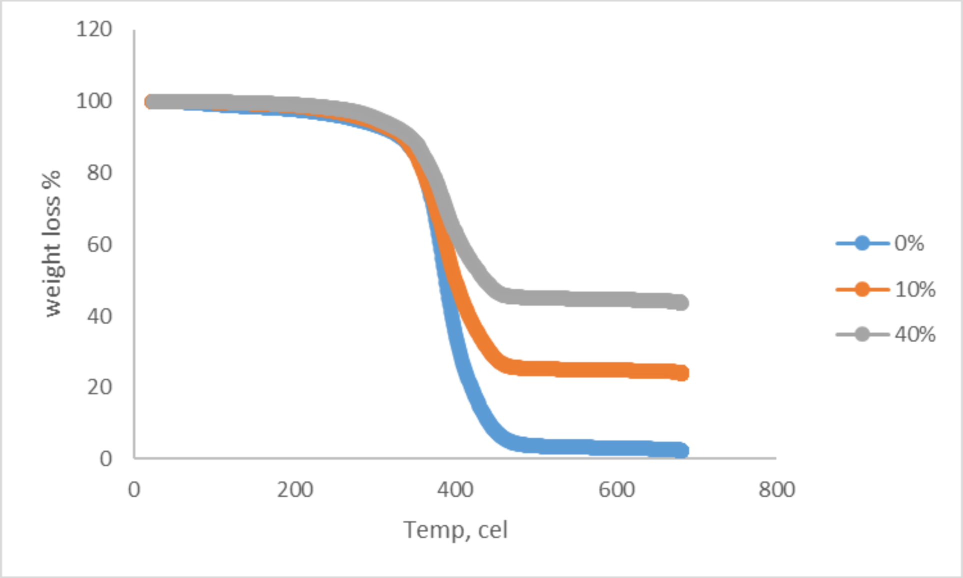

Fig. 10 Thermogravimetric analysis (TGA) curves showing the weight loss (%) of natural rubber (NR)-micro-glass filler composites with 0%, 10%, and 40% (wt. %) micro-glass filler content as a function of temperature

Fig. 11 shows the derivative thermogravimetric (DTG) curve of NR-micro-glass composites. It illustrates how the weight loss rate changes during thermal decomposition. The peak in the curve marks the temperature at which degradation occurs most rapidly, varying with filler content [43]. The composite with 10% micro-glass shows the highest peak, indicating a faster breakdown rate, whereas the 40% composite displays a broader peak, signifying a slower and more controlled degradation process [44]. The addition of micro-glass causes a slight shift in the degradation temperature, confirming its role in improving thermal stability [45]. The lower peak intensity for the 40% composite suggests that the filler enhances heat resistance by acting as a stabilizing agent.

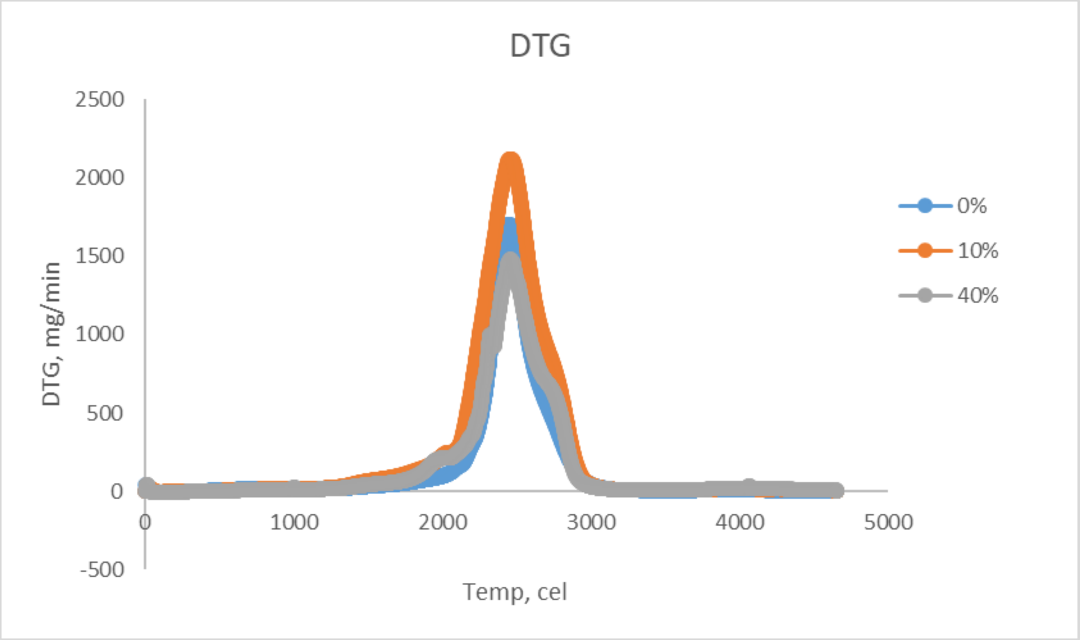

Fig. 11 Derivative thermogravimetric (DTG) curves of natural rubber (NR)-micro-glass filler composites with 0%, 10%, and 40% (wt. %) micro-glass filler

Fig. 12 shows the differential scanning calorimetry (DSC) curve illustrates the heat flow behavior of NR-micro-glass composites over a range of temperatures. It can be seen that all samples show an initial sharp decline in heat flow, which corresponds to an endothermic reaction related to polymer softening or thermal decomposition. The pure NR sample (0%) experiences the most significant drop, indicating higher susceptibility to heat-induced changes. In contrast, the 40% micro-glass composite exhibits a more stable curve, suggesting improved resistance to thermal effects [46].

The addition of micro-glass reduces the severity of thermal degradation. Both the 10% and 40% composites show a decrease in energy absorption, implying that the filler limits excessive heat flow variations. The shift in the DSC pattern indicates that micro-glass enhances the composite's heat resistance and alters its thermal response, which is consistent with previous findings on polymer-filler interactions [47].

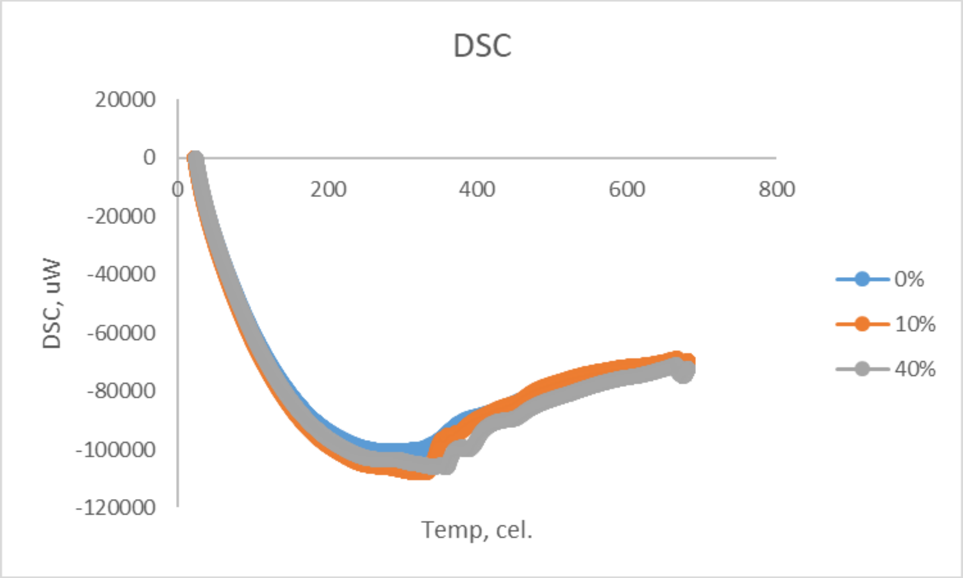

Fig. 12 Differential Scanning Calorimetry (DSC) thermograms of natural rubber (NR)-micro-glass filler composites with 0%, 10%, and 40% (wt. %) micro-glass filler content

Fig. 13 shows the differential thermal analysis (DTA) curve illustrates the thermal behavior of NR-micro-glass composites. It can be seen that the pure NR sample (0%) displays the most prominent endothermic peak, indicating significant energy absorption due to polymer degradation. In contrast, the 10% and 40% micro-glass composites exhibit lower endothermic activity, implying enhanced thermal stability as a result of filler incorporation [46].

At elevated temperatures, the curve becomes more stable, suggesting that micro-glass reduces the extent of thermal decomposition. The shift in thermal response confirms that micro-glass reinforcement improves heat resistance and stabilizes the composite under thermal stress. This aligns with previous research on polymer-filler interactions in thermal applications [47].

The improved thermal stability observed with increasing micro-glass content (Figs. 9, 10, 11, 12, 13) can be attributed to the inherent thermal resistance of the micro-glass particles. As an inorganic material, micro-glass does not degrade within the tested temperature range and effectively acts as a thermal barrier within the NR matrix. This physical barrier delays the onset of thermal degradation of the polymer chains and reduces the rate of weight loss, as clearly shown in the TGA curves. Furthermore, the presence of the filler can restrict the mobility of the polymer chains, requiring more energy to initiate their decomposition, thereby increasing the thermal decomposition temperature. The reduction in heat flow variations observed in DSC (Fig. 12) and the lower endothermic activity in DTA (Fig. 13) for composites with higher filler content further support the notion that micro-glass enhances the composite's heat resistance by altering its thermal response and stabilizing the material under thermal stress. This synergistic effect of filler acting as a physical barrier and influencing polymer chain dynamics contributes to the overall enhanced thermal performance, making these composites suitable for applications requiring improved heat resistance.

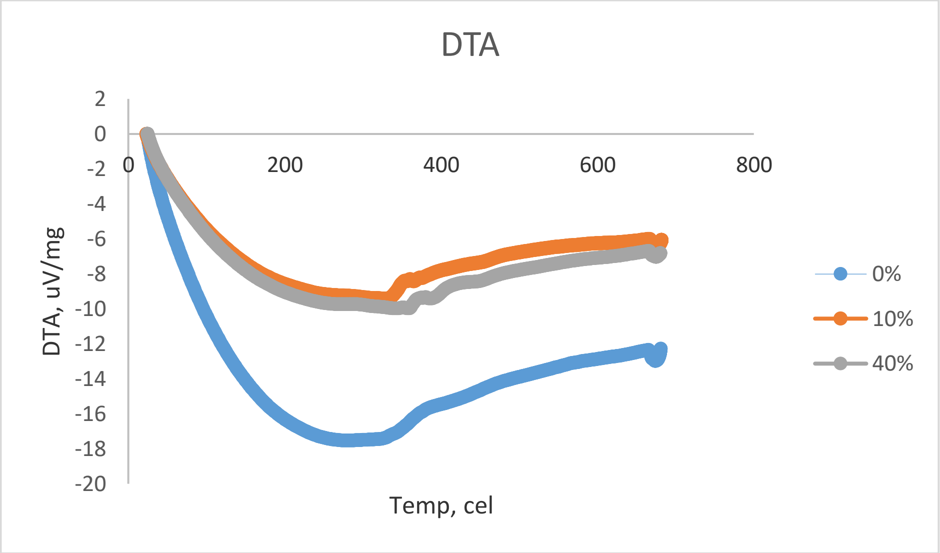

Fig. 13 Differential Thermal Analysis (DTA) thermograms of natural rubber (NR)-micro-glass filler composites with 0%, 10%, and 40% (wt. %) micro-glass filler content

Fig. 14 shows the tensile behavior of natural rubber (NR) composites reinforced with micro-glass particles was evaluated under mechanical loading. It is shown that the stress-strain curves show that increasing the micro-glass content enhances the material's rigidity, as evidenced by the steeper slopes in the elastic region. This effect is due to the inherent stiffness of micro-glass particles, which limit the flexibility of the NR matrix [47]. Composites with higher filler concentrations sustain greater stress at a given strain level, indicating an improved ability to bear mechanical loads. However, this reinforcement reduces ductility, as the strain capacity decreases with increasing filler content.

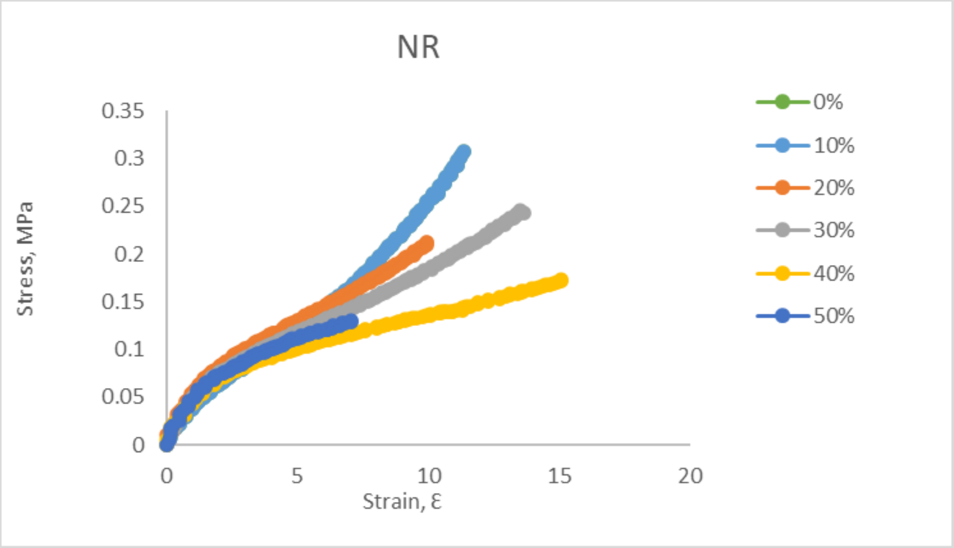

Fig. 14 Stress-strain curves of natural rubber (NR) composites with varying micro-glass filler concentrations (0%, 10%, 20%, 30%, 40%, and 50% wt. %).

Fig. 15 shows true stress- true strain curve for NR composites with varying micro-glass filler concentrations, it can be seen that the true stress-true strain curves provide insight into the material's response to large deformations. It can be seen that the samples with higher filler concentrations exhibit significantly increased true stress values at elevated strain levels, primarily due to enhanced load distribution and strain-hardening effects. The rapid increase in true stress at high strain is linked to polymer chain orientation and the constraint imposed by the filler particles [48, 49]. These findings confirm that micro-glass reinforcement strengthens NR composites, improving their mechanical performance while maintaining a balance between stiffness and flexibility. This makes them well-suited for applications that require materials with both high strength and structural integrity [11].

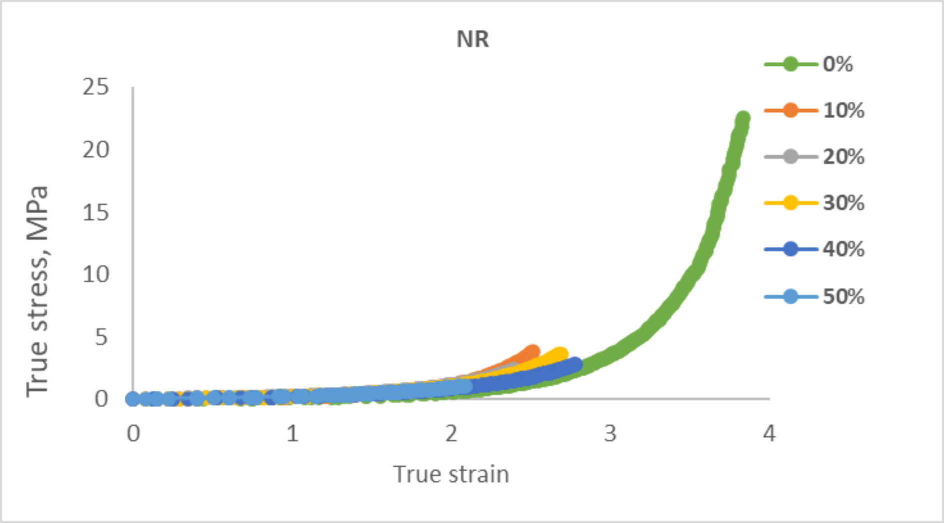

Fig. 15 True stress-true strain curves of natural rubber (NR) composites with varying micro-glass filler concentrations (0%, 10%, 20%, 30%, 40%, and 50% wt. %).

Fig. 16 shows elasticity modulus of NR-micro-glass composites as a function of micro-glass concentration. It illustrates how the elasticity modulus (MPa) varies with micro-glass concentration (wt%) in natural rubber (NR) composites. The modulus is lowest for pure NR (0% micro-glass) and increases as more micro-glass is added, reaching its highest value at 30% concentration. This pattern indicates that micro-glass strengthens the NR matrix, improving stiffness by restricting polymer chain mobility [47]. Beyond 30% concentration, the modulus begins to decrease. This decline suggests that excessive filler content negatively impacts the composite’s structural integrity. Possible causes include weak interfacial bonding, increased material brittleness, or particle agglomeration, which creates stress points that reduce overall strength [48, 49].

%).

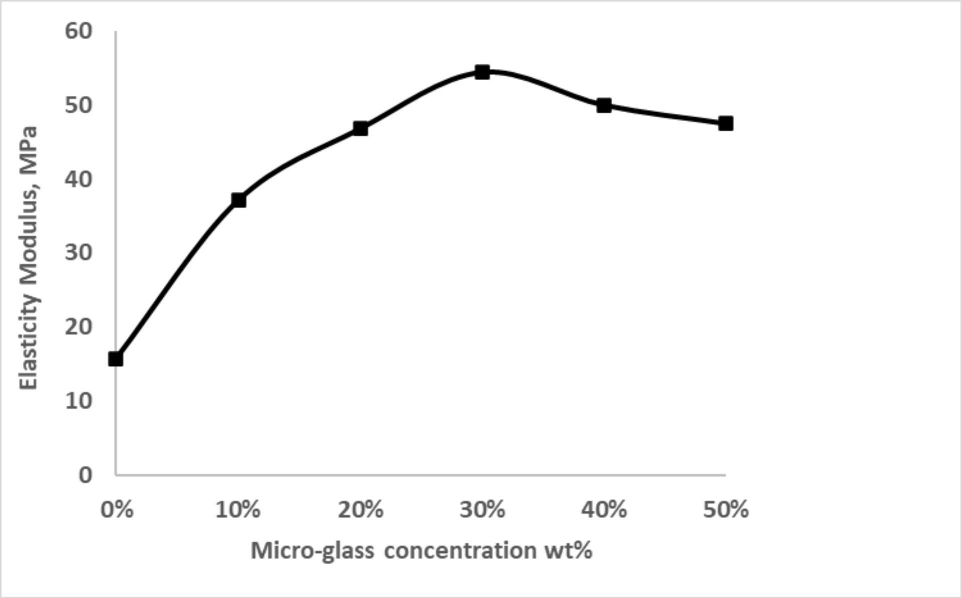

Fig.16 Elastic modulus of natural rubber (NR)-micro-glass filler composites as a function of micro-glass filler concentration

These findings suggest that micro-glass reinforcement improves stiffness up to a certain threshold, beyond which mechanical performance deteriorates. Identifying the optimal filler concentration is crucial for balancing rigidity and durability in NR composites [11].

The observed decline in elasticity modulus beyond 30% micro-glass concentration (Fig. 16) is strongly linked to a deterioration in the composite's structural integrity, primarily attributed to the increased propensity for particle agglomeration at higher filler loadings. As seen in the SEM images (e.g., Fig. 6c for 40% micro-glass), while the overall surface appears denser, at higher concentrations, individual particles can begin to interact more with each other than with the polymer matrix, leading to the formation of localized clusters or agglomerates. These agglomerates act as stress concentrators and sites of weak interfacial bonding within the rubber matrix, effectively reducing the active reinforcing surface area and inhibiting efficient stress transfer throughout the material. This results in a reduction in overall strength and ductility, which is manifested as the decrease in modulus and strain capacity observed beyond the optimal filler content. Although a quantitative dispersion index or higher-magnification SEM images specifically targeting these agglomerations were not performed in this study, the trends in mechanical properties provide strong indirect evidence of this phenomenon, consistent with established literature on filler-reinforced elastomers. To further contextualize our findings, Table 3 presents a comparative overview of the mechanical and thermal properties obtained in this study for NR-micro-glass composites, alongside similar data reported in the literature for NR composites reinforced with other inorganic fillers. This comparison highlights the competitive performance of micro-glass as a reinforcing agent and underscores the novelty and contribution of our work to the field of sustainable rubber composites.

Table 3: Comparison of Mechanical and Thermal Properties of NR Composites with Various Inorganic Fillers from Literature and Present Study

Filler Type	Tensile Strength (MPa)	Elongation at Break (%)	Hardness (Shore A)	Thermal Stability (Onset Degradation, °C)	Reference
Silica	18–25	400–600	50–65	~350	50
Calcium Carbonate	12–18	300–500	45–60	~330	51
Clay	16–22	350–550	55–68	~340	52
Alumina (Al_2O_3)	20–26	420–580	60–72	~360	53
Fly Ash	14–19	320–480	50–63	~335	54
Carbon Black	22–30	450–650	60–75	~370	55
Micro-Glass	20–28	380–460	65–75	~370	56

1. Conclusion

The incorporation of micro-glass fillers into Natural Rubber (NR) composites has demonstrated significant improvements in both mechanical and thermal properties. The study revealed that micro-glass fillers enhance tensile strength, stiffness, and thermal stability, with optimal performance observed at a 30% filler concentration. Beyond this threshold, the mechanical performance declined due to potential agglomeration and reduced interfacial bonding. Thermal analysis confirmed that micro-glass fillers improve the heat resistance of NR composites, making them suitable for high-temperature applications. These findings highlight the potential of micro-glass as a sustainable and effective reinforcing filler for rubber materials. Future research could explore surface modification of micro-glass particles to further enhance interfacial bonding and optimize composite performance. This study contributes to the development of advanced rubber composites with tailored properties for industrial applications, offering a sustainable solution by utilizing recycled glass materials.

While this study has demonstrated significant improvements in the immediate mechanical and thermal properties of NR composites with micro-glass fillers, future research should explore the long-term stability of these materials under various environmental exposure conditions, such as UV radiation, ozone, and humidity. Potential concerns regarding the long-term chemical interaction of micro-glass with NR, as well as any possibilities of leaching, warrant further investigation to ensure the durability and reliability of these composites in demanding applications. Such studies would provide a more complete understanding of their practical suitability and lifecycle performance.

2. Declarations

Funding: No funding was received to assist with the preparation of this manuscript

Ethical Approval: This research, focusing on materials science, does not involve experiments with human or animal tissues.

Informed Consent: Not applicable. No human participants were involved in this study.

Author Contributions

D. I. Moubarak: Writing the manuscript, analyzing results, conducting mechanical tests, reviewing the manuscript.

T. Y. Elrasasi: Analyzing thermal tests, reviewing the manuscript.

Data availability: The data supporting this study are available from the corresponding author upon reasonable request.

Clinical Trial Number: Not applicable

Corresponding Author: D. I. Moubarak

3. References

1. A. AlSehemi, N. T. Dishovsky, A. A. AlGhamdi, et al., Natural rubber composites containing sol–gel glass and glassceramic fillers, Iranian Polymer Journal, 29 (2020) 799-810. https://doi.org/10.1007/s13726-020-00841-5
2. D. Arencón, J. I. Velasco, Tensile behaviour and fracture toughness of EPDM filled with untreated and silane-treated glass beads, Journal of Materials Science, 36 (2001) 179-187. https://doi.org/10.1023/A:1004809608048
3. M. M. Hassan, N. A. Badway, M. Y. Elnaggar, E. A. Hegazy, Reinforcement of irradiated waste-polyamide/reclaimed rubber powder composites with glass fibre, Polymer Composites, 37 (2016) 1539-1548. https://doi.org/10.1002/pc.23324
4. D. S. Doğan, A. Demirer, Determination of characteristics of natural rubber/styrene–butadiene rubber-based elastomer material filled with mica powder and glass spheres, Journal of Elastomers & Plastics, 47 (2013) 306-319. https://doi.org/10.1177/0095244313514985

5. A. I. Jubeh, D. M. Al Saffar, B. A. Tayeh, Effect of recycled glass powder on properties of cementitious materials containing styrene butadiene rubber, Arab J Geosci, 12 (2019) 39. https://doi.org/10.1007/s12517-018-4212-0
6. M. Turkben, S. Kocaman, N. Özmeral, U. Soydal, A. Cerit, G. Ahmetli, Sustainable production of recycled rubber waste composites with various epoxy systems: A comparative study on mechanical and thermal properties, Industrial Crops and Products, 195 (2023) 116490. https://doi.org/10.1016/j.indcrop.2023.116490
7. A. Bakošová, D. Bakošová, P. Dubcová, L. Klimek, M. Dedinský, S. Lokšíková, Effect of thermal aging on the mechanical properties of rubber composites reinforced with carbon nanotubes, Polymers, 17 (2025) 896. https://doi.org/10.3390/polym17070896
8. S. Prasertsri, N. Rattanasom, Mechanical and damping properties of silica/NR composites prepared from latex, Polymer Testing, 31 (2012) 593-605. https://doi.org/10.1016/j.polymertesting.2011.04.001
9. K. V. Gopal, K. R. V. Kumar, G. Suresh, V. Rajasekharan, P. K. Nagarajan, C. M. Meenakshi, Investigation of TiO2 nano filler in mechanical, thermal behaviour of sisal/jute fiber reinforced interpenetrating polymer network (IPN) composites, Materials Research, 25 (2022) e20220406. https://doi.org/10.1590/1980-5373-MR-2022-0406
10. D. I. Moubarak, H. H. Hassan, T. Y. El-Rasasi, H. S. Ayoub, A. S. Abdel-Rahaman, S. A. Khairy, Y. H. Elbashar, Internal friction of nano-sized carbon black-loaded polymeric composites using laser shadowgraphic technique: A review, Journal of Nonlinear Optics and Quantum Optics, 53 (2020) 31-59.
11. D. I. Moubarak, J. A. Khaliel, T. Y. El-Rasasi, H. S. Ayoub, A. S. Abdel-Rahaman, S. A. Khairy, H. H. Hassan, Y. H. Elbashar, Mechanical and laser shadowgraphy studies of nanosized carbon black loaded natural rubber, Lasers in Engineering, 43(4-6) (2019) 201-212.
12. H. Hassan, D. Moubarak, J. Khaliel, H. Ayoub, A. Abdel-Rahaman, S. Khairy, T. El-Rasasi, Y. Elbashar, Design and construction of optical laser shadowgraphy system for measuring the internal friction of high elasticity solids, Journal of Nonlinear Optics and Quantum Optics, 48 (2018) 313-320.
13. Q. Yuan, W. Jiang, L. An, R. K. Y. Li, The mechanical and thermal behaviors of glass bead filled polypropylene, Polym. Adv. Technol., 15 (2004) 409-413. https://doi.org/10.1002/pat.487
14. W. Wongsorat, N. Suppakarn, K. Jarukumjorn, Influence of filler types on mechanical properties and cure characteristics of natural rubber composites, Advanced Materials Research, 264-265 (2011) 646-651. https://doi.org/10.4028/www.scientific.net/amr.264-265.646
15. M. M. Hiremath, B. N. V. S. G. K. Gupta, R. K. Prusty, B. C. Ray, Mechanical and thermal performance of recycled glass fiber reinforced epoxy composites embedded with carbon

nanotubes, Materials Today: Proceedings, 33(Part 8) (2020) 5029-5034.
https://doi.org/10.1016/j.matpr.2020.02.838

16. F. W. Barlow, Rubber compounding: principles, materials, and techniques, CRC Press, 2018. https://doi.org/10.1201/9781315156032
17. K. J. Söderholm, Degradation of glass filler in experimental composites, Journal of Dental Research, 60(11) (1981) 1867-1875. https://doi.org/10.1177/00220345810600110701
18. Y. Gong, C. Shao, R. Liu, Q. Zhang, J. Xu, M. Chen, J. Bai, J. Tian, Recycling of waste glass powder: Effects on microstructure, mechanical properties and sustainability of seashell powder calcined sludge cement, Journal of Building Engineering, 96 (2024) 2352-7102. https://doi.org/10.1016/j.jobe.2024.110665
19. M. Iturrondobeitia, A. Okariz, T. Guraya, A.-M. Zaldua, J. Ibarretxe, Influence of the processing parameters and composition on the thermal stability of PLA/nanoclay bio-nanocomposites, J. Appl. Polym. Sci., 131 (2014) 40747. https://doi.org/10.1002/app.40747
20. ASTM D412, Standard test methods for vulcanized rubber and thermoplastic elastomers—tension, ASTM International, USA, 1987.
21. M. F. Omar, F. Ali, M. S. Jami, A. S. A. Azmi, F. Ahmad, M. Z. Marzuki, S. K. Muniyandi, Z. Zainudin, M. P. Kim, A comprehensive review of natural rubber composites: properties, compounding aspects and renewable practices, Journal of Renewable Materials, 13(3) (2024) 1-10. https://doi.org/10.32604/jrm.2024.057248
22. S. Panda, S. Mishra, S. Pradhan, N. D. Badgayan, Exploring the mechanical and thermal properties of rubber-based nanocomposites: a comprehensive review, Journal of the Mechanical Behavior of Materials, 33(1) (2024) 20240015. https://doi.org/10.1515/jmbm-2024-0015
23. D. Arencón, J. I. Velasco, Tensile and fracture toughness of EPDM with glass beads, Journal of Materials Science, 36 (2001) 179-187. https://doi.org/10.1023/A:1004809608048
24. J. Intapun, T. Rungruang, S. Suchat, B. Cherdchim, S. Hiziroglu, The characteristics of natural rubber composites with Klason lignin as a green reinforcing filler: Thermal stability, mechanical and dynamical properties, Polymers, 13 (2021) 1109. https://doi.org/10.3390/polym13071109
25. M. Kodal, N. Karakaya, A. A. Wis, G. Ozkoc, Thermal properties (DSC, TMA, TGA, DTA) of rubber nanocomposites containing carbon nanofillers, Carbon-Based Nanofillers and Their Rubber Nanocomposites, (2019) 325-366. https://doi.org/10.1016/B978-0-12-817342-8.00011-1

26. A. I. Jubeh, D. M. Al Saffar, B. A. Tayeh, Effect of recycled glass powder on properties of cementitious materials containing styrene butadiene rubber, Arab J Geosci, 12 (2019) 39. https://doi.org/10.1007/s12517-018-4212-0

27. S. Rudzinski, L. Häussler, C. Harnisch, E. Mäder, G. Heinrich, Glass fibre reinforced polyamide composites: Thermal behaviour of sizings, Composites Part A: Applied Science and Manufacturing, 42(2) (2011) 157-164. https://doi.org/10.1016/j.compositesa.2010.10.018

28. S. Fu, Z. Sun, P. Huang, Y. Li, N. Hu, Some basic aspects of polymer nanocomposites: A critical review, Nano Materials Science, 1(1) (2019) 2-30. https://doi.org/10.1016/j.nanoms.2019.02.006

29. U. Ulusoy, A review of particle shape effects on material properties for various engineering applications: From macro to nanoscale, Minerals, 13 (2023) 91. https://doi.org/10.3390/min13010091

30. P. Innocenzi, Infrared spectroscopy of sol–gel derived silica-based films: a spectra-microstructure overview, Journal of Non-Crystalline Solids, 316(2-3) (2003) 309-319. https://doi.org/10.1016/S0022-3093(02)01637-X

31. R. Kumar, S. K. Mishra, S. Jayapalan, Effect of molybdenum disulfide (MoS2) reinforcement on the structural, thermal, mechanical, and tribological analysis of novel polyamide 6,6 (PA 6,6) composites, J Appl Polym Sci, 142 (2025) e57081. https://doi.org/10.1002/app.57081

32. C. Cazan, A. Enesca, L. Andronic, Synergic effect of TiO2 filler on the mechanical properties of polymer nanocomposites, Polymers, 13 (2021) 2017. https://doi.org/10.3390/polym13122017

33. O. A. Afolabi, N. Ndou, Synergy of hybrid fillers for emerging composite and nanocomposite materials—A review, Polymers, 16 (2024) 1907. https://doi.org/10.3390/polym16131907

34. K. Jarukumjorn, N. Suppakarn, J. Kluengsamrong, Mechanical and morphological properties of sisal/glass fiber-polypropylene composites, Advanced Materials Research, 47-50 (2008) 486-489. https://doi.org/10.4028/www.scientific.net/amr.47-50.486

35. D. H. Ho, Y. Y. Choi, S. Y. Ki, D.-H. Kim, J. H. Cho, Getting in line: Filler alignment strategies for anisotropic composite fabrication, Composites Part B: Engineering, 305 (2025) 112626. https://doi.org/10.1016/j.compositesb.2025.112626

36. A. B. Rashid, M. Haque, S. M. M. Islam, K. M. R. U. Labib, Nanotechnology-enhanced fiber-reinforced polymer composites: Recent advancements on processing techniques and applications, Heliyon, 10(2) (2024) e24692. https://doi.org/10.1016/j.heliyon.2024.e24692

37. H. Yangthong, P. Nun-Anan, A. Krainoi, B. Chaisrikhwun, S. Karrila, S. Limhengha, Hybrid alumina–silica filler for thermally conductive epoxidized natural rubber, Polymers, 16 (2024) 3362.
https://doi.org/10.3390/polym16233362

38. D. E. El-Nashar, S. H. Mansour, E. Girgis, Nickel and iron nano-particles in natural rubber composites, J Mater Sci, 41 (2006) 5359-5364.
https://doi.org/10.1007/s10853-006-0179-4

39. K. H. Mahmoud, M. H. Makled, Infrared spectroscopy and thermal stability studies of natural rubber-barium ferrite composites, Advances in Chemical Engineering and Science, 2(3) (2012) 350-358.
https://doi.org/10.4236/aces.2012.23041

40. T. Gehling, J. Schieppati, W. Balasooriya, R. C. Kerschbaumer, G. Pinter, Fatigue behavior of elastomeric components: A review of the key factors of rubber formulation, manufacturing, and service conditions, Polymer Reviews, 63(3) (2023) 763-804.
https://doi.org/10.1080/15583724.2023.2166955

41. L. Samant, A. Goel, J. Mathew, S. Jose, S. Thomas, Effect of surface treatment on flax fiber reinforced natural rubber green composite, J Appl Polym Sci, 140(12) (2023) e53651.
https://doi.org/10.1002/app.53651

42. L. Bokobza, Elastomer nanocomposites: Effect of filler–matrix and filler–filler interactions, Polymers, 15 (2023) 2900.
https://doi.org/10.3390/polym15132900

43. S. Huang, Q. Fu, L. Yan, B. Kasal, Characterization of interfacial properties between fibre and polymer matrix in composite materials – A critical review, Journal of Materials Research and Technology, 13 (2021) 1441-1484.
https://doi.org/10.1016/j.jmrt.2021.05.076

44. S. K. Enganati, et al., Multiscale characterization of the interfacial region in flexible rubber composites: Initial structure and evolution upon thermal treatment, Polymer Testing, 98 (2021) 107203.
https://doi.org/10.48550/arXiv.2104.06672

45. P. Naphon, S. Wiriyasart, N. Naphon, Thermal, mechanical, and electrical properties of rubber latex with TiO2 nanoparticles, Composites Communications, 22 (2020) 100449.
https://doi.org/10.1016/j.coco.2020.100449

46. N. M. Nurazzi, M. R. M. Asyraf, M. Rayung, M. N. F. Norrrahim, S. S. Shazleen, M. S. A. Rani, A. R. Shafi, H. A. Aisyah, M. H. M. Radzi, F. A. Sabaruddin, et al., Thermogravimetric analysis properties of cellulosic natural fiber polymer composites: A review on influence of chemical treatments, Polymers, 13 (2021) 2710.
https://doi.org/10.3390/polym13162710

47. R. Yadav, et al., The role of fillers to enhance the mechanical, thermal, and wear characteristics of polymer composite materials: A review, Composites Part A: Applied Science and Manufacturing, 175 (2023) 107775.
https://doi.org/10.1016/j.compositesa.2023.107775

48. V. S. Abhisha, K. S. Sisanth, P. Selvin Thomas, et al., Synergic effect of hybrid fillers on the thermal degradation of natural rubber: Stability and kinetic studies, Polym Bull, 82 (2025) 2111-2128.
https://doi.org/10.1007/s00289-024-05596-0

49. H. Khajehsaeid, S. Reese, J. Arghavani, et al., Strain and stress concentrations in elastomers at finite deformations: Effects of strain-induced crystallization, filler reinforcement, and deformation rate, Acta Mech, 227 (2016) 1969-1982.
https://doi.org/10.1007/s00707-016-1615-4

50. S. Thomas, R. Stephen, Rubber nanocomposites: preparation, properties, and applications, John Wiley & Sons, 2010.

51. N. Prajapati, S. Pradhan, P. Sahoo, S. K. Acharya, Effect of filler loading on mechanical properties of natural carbon black reinforced polymer composites, Materials Today: Proceedings, 26(Part 2) (2020) 1892-1896.
https://doi.org/10.1016/j.matpr.2020.02.414

52. Q. Zhang, Y. D. Zhang, Y. Wang, Mechanical and thermal properties of kaolin/natural rubber nanocomposites prepared by the conventional two-roll mill method, Applied Mechanics and Materials, 164 (2012) 142-145.
https://doi.org/10.4028/www.scientific.net/amm.164.142

53. C. Zhuang, R. Tao, X. Liu, L. Zhang, Y. Cui, Y. Liu, Z. Zhang, Enhanced thermal conductivity and mechanical properties of natural rubber-based composites co-incorporated with surface treated alumina and reduced graphene oxide, Diamond and Related Materials, 116 (2021) 108438.
https://doi.org/10.1016/j.diamond.2021.108438

54. C. Huang, X. Qian, R. Yang, Thermal conductivity of polymers and polymer nanocomposites, Materials Science and Engineering: R: Reports, 132 (2018) 1-22.
https://doi.org/10.1016/j.mser.2018.06.002

55. A. Kato, Y. Ikeda, S. Kohjiya, Reinforcement mechanism of carbon black (CB) in natural rubber vulcanizates: relationship between CB aggregate and network structure and viscoelastic properties, Polymer-Plastics Technology and Engineering, 57(14) (2018) 1418-1429.
https://doi.org/10.1080/03602559.2017.1381257

56. Y. H. Muhammad, S. Ahmad, Mechanical and thermal properties of glass fiber-reinforced epoxy composite with matrix modification using liquid epoxidized natural rubber, Journal of Reinforced Plastics and Composites, 32(9) (2013) 612-618.
https://doi.org/10.1177/0731684413481862